The Chiral Molecule CHClFI: First Determination of Its Molecular Parameters by Fourier Transform Microwave and Millimeter-Wave Spectroscopies Supplemented by ab Initio Calculations

A. Cuisset,*,† J. R. Aviles Moreno,† T. R. Huet,† D. Petitprez,† J. Demaison,† and J. Crassous‡

Laboratoire de Physique des Lasers, Atomes et Molécules (PhLAM) UMR 8523 CNRS-Université de Lille 1, 59655 Villeneuve d'Ascq Cedex, France, and Laboratoire de Chimie, Unité mixte CNRS-ENS Lyon 5182, 46 Allée d'Italie, 69364 Lyon Cedex 07, France

Received: December 10, 2004; In Final Form: May 4, 2005

The rotational spectrum of chlorofluoroiodomethane (CHClFI) has been investigated. Because its rotational spectrum is extremely crowded, extensive ab initio calculations were first performed in order to predict the molecular parameters. The low *J* transitions were measured using a pulsed-molecular-beam Fourier transform spectrometer, and the millimeter-wave spectrum was measured to determine accurate centrifugal distortion constants. Because of the high resolution of the experimental techniques, the analysis yielded accurate rotational constants, centrifugal distortion corrections, and the complete quadrupole coupling tensors for the iodine and chlorine nuclei, as well as the contribution of iodine to the spin−rotation interaction. These molecular parameters were determined for the two isotopologs $CH^{35}ClFI$ and $CH^{37}ClFI$. They reproduce the observed transitions within the experimental accuracy. Moreover, the ab initio calculations have provided a precise equilibrium molecular structure. Furthermore, the ab initio molecular parameters are found in good agreement with the corresponding experimental values.

Introduction

Chiral compounds are currently being investigated in order to observe a parity violation effect in a molecule. The most recent theoretical calculations and experiments aim at demonstrating any spectroscopically measurable energy differences between the *S* and *R* enantiomeric states of chiral molecules. Using a fully relativistic formalism, the group of Schwerdtfeger recently pointed out the importance of the vibrational anharmonicity contributions.[1] Subsequently, a small number of chiral molecules were theoretically investigated in order to predict the magnitude of the parity violation effects. Four CFXYZ compounds (X, Y, Z = H, Cl, Br, I) were considered, and the differences in frequency were found to be the highest for the C−F stretching fundamental transitions (1.7 mHz for CHBrClF, 11.6 mHz for CBrClFI, 23.7 mHz for CHClFI, and 50.8 mHz for CHBrFI).[2] The choice to study this type of molecules was motivated by the pioneering work of Bauder and co-workers[3], who fully characterized the pure rotation and the C−F infrared spectra of CHBrClF. Unfortunately, the saturation spectroscopy experiment subsequently performed on CHBrClF in the group of Chardonnet and co-workers was not capable of reaching millihertz accuracy, and the test was unsuccessful.[4,5] Quack and Stohner recently investigated the isotopolog CDBrClF.[6] They developed a multidimensional approach, combining the CD and CF chromophore subspaces, and analyzed in detail the accuracy of relativistic calculations. However, because of the limited resolution of experimental setups, the parity violation effects must be explored on molecules containing heavier atoms, like chlorofluoroiodomethane CHClFI;[7] therefore, such a methyl halide is a good candidate and must be spectroscopically characterized.

We report in this paper the successful synthesis of CHClFI (Figure 1) and the first spectroscopic characterization of this stable molecule. It has small rotational constants and no symmetry. Furthermore, two of its atoms (Cl and I) induce a complex hyperfine structure of the rotational lines. Two isotopologs (due to ^{35}Cl and ^{37}Cl) are present in the sample. Finally, the first excited vibrational states are rather low. For all these reasons, the rotational spectrum is extremely crowded. To be able to analyze it, extensive ab initio calculations were performed to predict the molecular parameters (rotational constants, dipole moment, quadrupole coupling constants, and centrifugal distortion constants). Then, low *J* transitions were recorded using a pulsed-molecular-beam Fourier transform microwave (FTMW) spectrometer in the gigahertz range. The supersonic beam cools the gas to a few Kelvin, which considerably reduces the number of observable transitions. Finally, the millimeter-wave (MMW) spectrum was measured to determine accurate centrifugal distortion constants. All the determined molecular parameters (especially the hyperfine constants) are essential for the assignment of the ultrahigh-resolution infrared spectrum. Finally, a detailed discussion on the nature of quadrupolar coupling is presented.

Experimental Section

Samples. The synthesis of racemic chlorofluoroiodomethane (±)-CHClFI **1**, described in Figure 2, was performed in Lyon. Racemic chlorofluoroiodoacetic acid ((±)-FClIC−CO_2H) **2** was first synthesized in four steps from chlorotrifluoroethylene, as described recently.[8] Then, its strychninium salt was decarboxy-

* To whom correspondence should be addressed. Present address: Laboratoire de Physico-Chimie de l'Atmosphère CNRS UMR 8101, Université du Littoral Côte d'Opale, 189 A Ave. Maurice Schumann 59140 Dunkerque, France. E-mail: arnaud.cuisset@univ-littoral.fr.

† Laboratoire de Physique des Lasers, Atomes et Molécules (PhLAM) UMR 8523 CNRS-Université de Lille 1.

‡ Laboratoire de Chimie, Unité mixte CNRS-ENS Lyon 5182.

10.1021/jp0443658 CCC: $30.25
Published on Web 06/04/2005

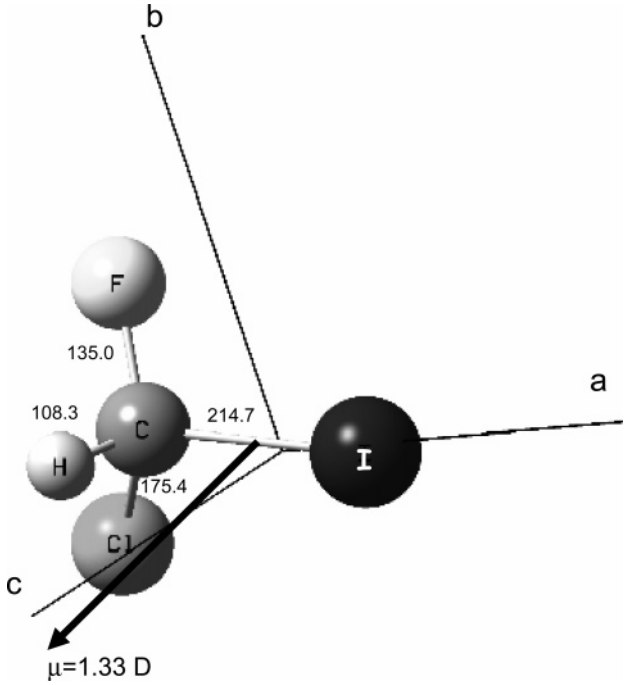

Figure 1. Ab initio calculated structure, principal axes *a*, *b*, and *c* and electric dipole moment $\vec{\mu}$ of CHClFI (MP2/SDB-VTZ, see Table 3). The bond lengths are in picometers and the dipole moment in debye. The origin of the dipole moment vector was placed at the center of the positive nuclear charges.

lated into (±)-CHClFI, as follows: 19.9 g (3.47 mmol) of the strychninium salt of **2** ((±)-FClIC−CO_2H, (−)-strychnine) was heated at 110 °C, and 110 mm Hg in triethylene glycol (70 mL) for 1 h. (±)-CHClFI was collected as a colorless liquid in a cold trap at −78 °C (2.382 g, 35%). The NMR parameters used for the synthesis are identical to those in literature:[9] ^{1}H NMR ($CDCl_3$, 200 MHz) δ 7.62 (d, $^2J_{HF}$ = 50.2 Hz); ^{13}C NMR ($CDCl_3$, 50.4 MHz) δ 55.04 (d, $^1J_{CF}$ = 308.4 Hz); ^{19}F NMR ($CDCl_3$, 188.2 MHz, $CFCl_3$ as internal reference) δ −86.99 (d, $^2J_{HF}$ = 50.2 Hz); and ^{19}F NMR ($CDCl_3$, 188.2 MHz, CF_3CO_2H as internal reference) δ −11.03 (d, $^2J_{HF}$ = 50.3 Hz).

Fourier Transform Microwave Spectrometer. Rotational spectra in the 6−20 GHz spectral range were recorded using the Lille FTMW spectrometer.[10] A gas mixture of 3 mbar of CHClFI completed with neon as the carrier gas to a total pressure of 1 bar was prepared. Gas pulses were then expanded into the vacuum tank through a pulsed nozzle to create a supersonic beam. As the nozzle is inserted in the center of the fixed mirror of the Fabry−Perot cavity, the supersonic expansion is parallel to the optical axis of the cavity. Each transition is divided into two Doppler components. A complex rotational spectrum was expected because of the large hyperfine structure caused especially by the iodine atom and the presence of two isotopologs, $CH^{37}ClFI$ and $CH^{35}ClFI$ for which the natural abundance is in the ratio 1:3. Large spectral region surveys were conducted from 7 to 16 GHz, using the fast (low-resolution) scan mode facilities of the spectrometer. In this operating mode, around 10 free induction decays were averaged and Fourier transformed at a repetition rate of 1.5 Hz. Two data points are then collected from the frequency domain signal, namely, the maximum intensity of the spectrum and the corresponding frequency. This operation is then automatically repeated every 0.4 MHz, which corresponds to the bandwidth of the Fabry−Perot cavity, to cover step by step the whole desired frequency region. An example of such a collection of data in given in Figure 3 (scan around 7 GHz). Each molecular transition is then recorded with a higher frequency resolution. The central frequencies of the lines are determined by averaging the frequencies of the two Doppler components after transformation of 4096 data points time domain signal, leading to a digital resolution of 2.4 kHz in the spectrum. The accuracy of frequency measurements is estimated to be better than 3 kHz. The line width for a typical, well-resolved line is 10 kHz. Such a high-resolution spectrum is shown in Figure 4 (part of the $4_{13} \leftarrow 3_{03}$ transition around 17 GHz). The three μ_a, μ_b, and μ_c types of transitions have been observed. At the same microwave pulse length, the optimal microwave powers to polarize the molecules were found to be around 20 mW for μ_a and μ_b types of transitions and 4 mW for μ_c-type transitions, respectively (which indicates that $\mu_c > \mu_b \approx \mu_a$). All the FTMW data were weighted according to the frequency measurement accuracy.

Millimeter Spectra. To determine accurately the molecular parameters, rotational spectra were measured in the millimeter-wave range. Several high *J* lines of CHClFI have been observed at room temperature in the 270−350 GHz range and recorded at a pressure of about 0.13 mbar. All spectra were measured with the Lille computer-controlled MMW spectrometer using a phase-stabilized backward-wave-oscillator source and a He-cooled InSb bolometer (Queens Mary College) detector. The accuracy of the measurements is about 50 kHz. However, several lines are broadened by the quadrupole hyperfine structure or the *K* degeneracy and can only be resolved when the frequency difference reaches 400 kHz. All these blended lines were individually weighted (between 2 and 4 times the measurement accuracy) accordingly to the obsd−calcd values. This procedure

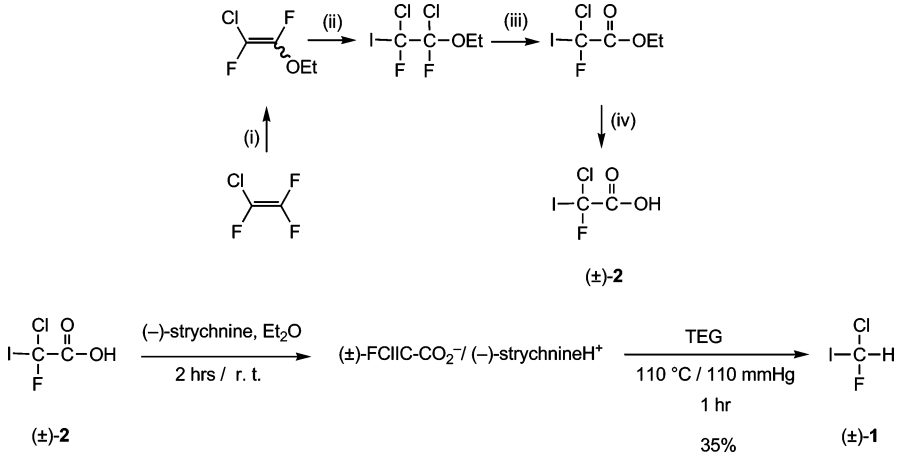

Figure 2. Synthesis of racemic CHClFI. (i) EtONa, Et_2O; (ii) ICl, CH_2Cl_2; (iii) concd H_2SO_4; (iv) aq NaOH then H_2SO_4.

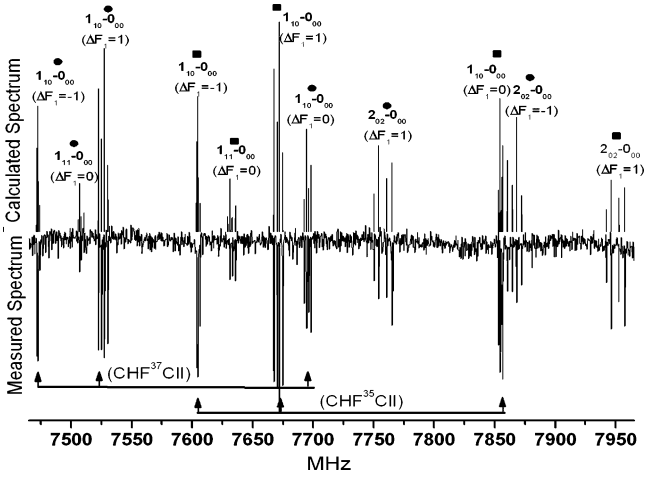

Figure 3. Wide frequency scan between 7465 and 7965 MHz showing the $1_{10} \leftarrow 0_{00}$, $1_{11} \leftarrow 0_{00}$, and $2_{02} \leftarrow 0_{00}$ transitions for both $CH^{35}ClFI$ (squares) and $CH^{37}ClFI$ (circles) isotopologs. Experimental conditions: 10 gas pulses per experiment; microwave pulses length, 2 μs; microwave power, 50 mW; gas pulse lengths, 700 μs. The arrows point to the iodine hyperfine structure of the $1_{10} \leftarrow 0_{00}$ transitions for $CH^{35}ClFI$ and $CH^{37}ClFI$.

was carefully applied in order to not bias the fit and for reaching frequencies as meaningful as possible.

Assignments and Analysis

Effective Hamiltonian. CHClFI is a near-prolate asymmetric top ($\kappa = -0.90$). The spectrum observed in the singlet ground electronic state was analyzed with a Hamiltonian model containing the molecular rotation and the associated centrifugal corrections terms, the nuclear quadrupole interaction effect for the iodine and chlorine nuclei, and the nuclear spin−rotation interaction associated with the iodine atom

$$\hat{H} = \hat{H}_R + \hat{H}_Q^{(I)} + \hat{H}_Q^{(Cl)} + \hat{H}_{CD} + \hat{H}_{NSR}^{(I)} \quad (1)$$

In eq 1, the five terms are ordered according to the magnitude of their energetic contribution. The rigid asymmetric rotor Hamiltonian H_R is written as[11]

$$\hat{H}_R = \left[A - \frac{1}{2}(B+C)\right]\hat{J}_z^2 + (B+C)\hat{J}^2 + \frac{1}{2}(B-C)(\hat{J}_x^2 - \hat{J}_y^2) \quad (2)$$

with $\hat{J}^2 = \hat{J}_x^2 + \hat{J}_y^2 + \hat{J}_z^2$. The I^r prolate representation was used, and A, B, and C are the principal rotational constants. H_{CD} denotes the centrifugal distortion terms of the Watson's A-reduced expression given by

$$\hat{H}_{CD} = -\Delta_J\hat{J}^4 - \Delta_{JK}\hat{J}^2\hat{J}_z^2 - \Delta_K\hat{J}_z^4 - \delta_K[\hat{J}_z^2, \hat{J}_x^2 - \hat{J}_y^2]_+ - 2\delta_J J^2(\hat{J}_x^2 - \hat{J}_y^2) + \Phi_K J_z^6 \quad (3)$$

The S-reduction was also tried but did not give better results. The two nuclear quadrupole interaction H_Q terms are written as[12]

$$\hat{H}_Q^{(N)} = \frac{1}{6}\sum_{i,j=x,y,z}\hat{Q}_{ij}^{(N)}\hat{V}_{ij}^{(N)} \quad N = I \text{ or } Cl \quad (4)$$

Equation 4 describes the interaction between the nuclear quadrupole electric moment $Q^{(N)}$ and the molecular electric field gradient $V^{(N)}$ for the nucleus N. The spectroscopic parameters are the elements of the quadrupole coupling tensor given by

$$\chi_{\alpha\beta}^{(N)} = eQ^{(N)}\frac{\partial^2 V^{(N)}}{\partial\alpha\,\partial\beta} \quad (5)$$

α and β refer to the coordinates a, b, and c of the principal inertial axes and e denotes the elementary charge. Only five parameters can be determined, that is, two diagonal elements and three off-diagonal elements, associated with the real symmetric traceless quadrupole coupling tensor. In the case of CHClFI, the five parameters must be determined to account for the observed structure. Finally, the observed hyperfine structure revealed a contribution from the nuclear spin−rotation inter-

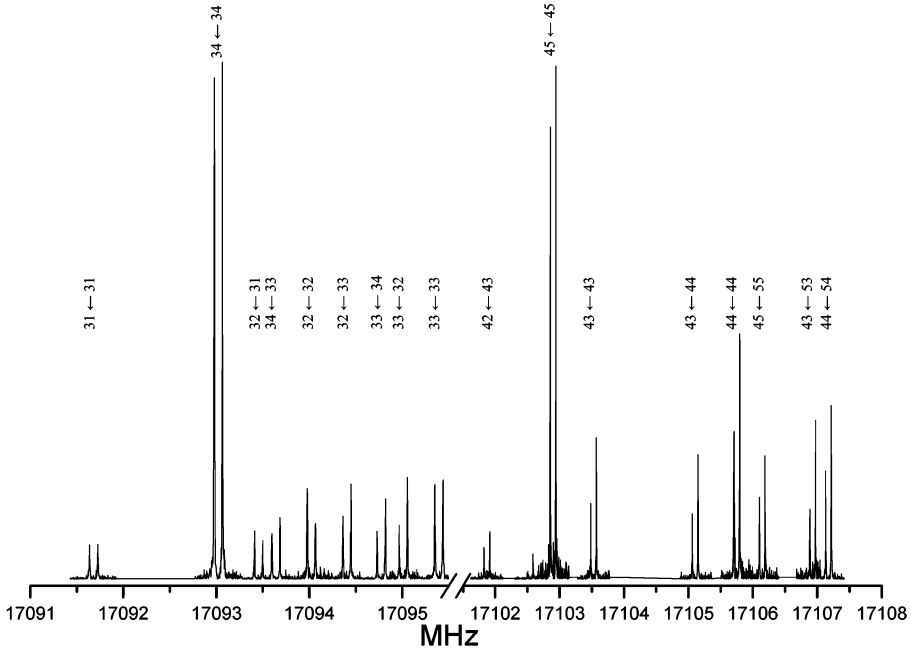

Figure 4. Part of the well-resolved $\Delta F_1 = 3 \leftarrow 3$ and $4 \leftarrow 4$ components of the $J_{KaKc} = 4_{13} \leftarrow 3_{03}$ transition. The figure is obtained by concatenation of several high-resolution spectra obtained after Fourier transformation of 100 coadded free induction decays.

action. The Hamiltonian term H_{NSR} is written as in refs 12−13

$$\hat{H}_{NSR} = \sum_i \mathbf{I}_i \cdot \mathbf{C}_i \cdot \mathbf{J} \quad (6)$$

where $\mathbf{C}_i$ is a second rank Cartesian tensor describing the spin−rotation coupling of the ith nuclei. Equation 6 can be written using the methods of irreductible tensors as

$$\hat{H}_{NSR} = \sum_i \sum_{k=0}^{2} N_k [\mathbf{C}_i^{(k)} \times \mathbf{J}^{(1)}]^{(1)} \times \mathbf{I}^{(1)} \quad (7)$$

where N_k are normalization factors and $[\mathbf{C}_i^{(k)} \times \mathbf{J}^{(1)}]^{(1)}$ are the irreductible products. The matrix elements can be evaluated using tensor algebra, giving rise to the spin−rotation constants (see ref 12 for details).

Determination of Molecular Parameters. Prior to the analysis, preliminary spectroscopic parameters were evaluated using the same basic procedure as in ref 3. First the rotational constants were calculated using the ab initio structural parameters (see Table 3). Then, the four bonds of the molecule, particularly C−I and C−Cl, were oriented using a rotation matrix with respect to the principal axes *a*, *b*, and *c*. To estimate the iodine and chlorine nuclear coupling constants, the assumption was made that in CHClFI the principal axes of $\chi^{(I)}$ and $\chi^{(Cl)}$ coincide with the C−I and C−Cl bonds, respectively. Then, the experimental diagonal quadrupole coupling tensors, $\chi^{(I)}$ from CH_3I[14] and $\chi^{(Cl)}$ from CH_3Cl,[15] oriented along the C−I and C−Cl bonds, respectively, were rotated to the principal inertial axis system of CHClFI. As an example, the five independent elements of $\chi^{(I)}$ for $CHFI^{35}Cl$ calculated by the rotation of the corresponding coupling tensor of CH_3I were $\chi_{aa} = -1625.1$ MHz, $\chi_{bb} = 801.7$ MHz, $\chi_{ab} = 654.6$ MHz, $\chi_{ac} = 610.0$ MHz, and $\chi_{bc} = -154.0$ MHz. These extrapolated tensors were used in the preliminary analysis.

The observed microwave spectrum was predicted and analyzed using the Pickett's program.[16] In CHClFI, the quadrupole interaction effect from the iodine nucleus ($Q^{(I)} = -0.710(10)$ Barn[17]) is larger than that for the chlorine nucleus ($Q^{(35Cl)} = -0.081\,65(80)$ Barn, $Q^{(37Cl)} = -0.064\,35(64)$ Barn[18]) by almost 1 order of magnitude. Consequently, we used the so-called sequential scheme for the addition of the angular momenta

$$\hat{J} + \hat{I}_I = \hat{F}_1 \qquad \hat{F}_1 + \hat{I}_{Cl} = \hat{F} \quad (8)$$

The angular momentum operators $\hat{I}_I$ and $\hat{I}_{Cl}$ are associated with the nuclear spins of the iodine ($I_I = {}^5/_2$) and chlorine ($I_{Cl} = {}^3/_2$) atoms, respectively. At low J values, both μ_b- and μ_c-type transitions were expected to occur in the same spectral region. Figure 3 illustrates the observed structure for the $1_{10} \leftarrow 0_{00}$ and $1_{11} \leftarrow 0_{00}$ transitions, labeled with the J_{KaKc} quantum numbers. For these transitions, the hyperfine splittings only concern the higher levels. The spectrum exhibits widely spaced triplet patterns due to the iodine hyperfine structure and associated with $\Delta F_1 = 0, \pm 1$. The sign of the diagonal elements $\chi_{bb}^{(I)}$ and $\chi_{cc}^{(I)}$ was readily determined. The detailed structure within each group of lines is associated with the $\Delta F = 0, \pm 1$ selection rules and is principally due to the chlorine hyperfine structure. Very similar patterns are observed for $CH^{35}ClFI$ and $CH^{37}ClFI$, which clearly facilitated the assignment. The detailed hyperfine structure of the $\Delta F_1 = 1$ components is also displayed in Figure 3. Moreover, a strong $2_{02} \leftarrow 0_{00}$ transition was observed. These $\Delta J = 2$ transitions may appear because the off-diagonal quadrupolar coupling elements of the iodine nucleus are large.[11,19] In our case, it is the coupling between the nearly degenerate levels 2_{02} and 1_{10} ($\Delta E \approx 300$ MHz) which is responsible for the borrowed intensity. All the *b*- and *c*-type $R(J)$ lines ($J = 0, 1$) were used to adjust the rotation constants and all the elements of $\chi^{(I)}$ and $\chi^{(35Cl)}$ or $\chi^{(37Cl)}$. The spectroscopic parameters were next refined by including weaker lines of higher J and K_a values. Although the hyperfine splitting patterns of these transitions were rather complex, particularly for the chlorine hyperfine components included inside every iodine hyperfine component, the assignment of the lines observed in the frequency region 11−17 GHz was straightforward. This is nicely illustrated in Figure 4 in the region of the rotational transition $4_{13} \leftarrow 3_{03}$ of $CH^{35}ClFI$. Details of the $\Delta F_1 = 3 \leftarrow 3$ transitions clearly show that all the chlorine hyperfine components were resolved and assigned. This is due to the very high resolution and sensitivity of the FTMW spectrometer.

Initially, 2 sets of 328 transitions for $CH^{35}ClFI$ and 140 transitions for $CH^{37}ClFI$ were assigned for $J < 5$, $K_a < 3$. As the quartic distortion parameters could not be accurately fitted, millimeter-wave data were recorded for the $CH^{35}ClFI$ isotopolog. 281 transitions have been assigned with $1 < K_a < 31$, $23 < J < 75$. The complete set of $CH^{35}ClFI$ transitions was fitted, and the spectroscopic parameters were obtained by a least-squares procedure.[16] The parameters are listed in Table 1 and reproduce the observed transitions with a standard deviation of 44 kHz. The unblended lines in the 6−20 GHz region are reproduced with a standard deviation of 2.3 kHz, within the experimental accuracy. The values of the distortion parameters for $CH^{37}ClFI$ were fixed to the corresponding $CH^{35}ClFI$ values. The molecular parameters presented in Table 1 reproduced the 140 fitted lines with a standard deviation of 2.1 kHz. It was found necessary to include in the fit the spin−rotation contribution from the iodine nucleus. However, the observed effects are within the experimental accuracy, and only the diagonal elements and the C_{ab} off-diagonal element of the iodine coupling tensor were fitted. Because of the correlation between constants, the other off-diagonal elements could not be experimentally determined. Consequently, the smaller spin-rotation effects (i.e., those associated with the hydrogen, fluorine, and chlorine atoms) were neglected. All the observed and calculated frequencies for the two chlorine isotopologs $CH^{35}ClFI$ and $CH^{37}ClFI$ are given in the Supporting Information.

Ab Initio Calculations

The objective of the ab initio calculations is twofold: First, they are used to predict molecular parameters as accurately as possible in order to facilitate the assignment of the spectrum; second, a structure as close as possible to the equilibrium structure is calculated. Accurate structures for molecules containing either bromine or chlorine are indeed scarce;[20] it would be extremely worthwhile to compare the structure of CHClFI to the structures of the methyl halides. The calculation of the equilibrium structure will be reported first.

All calculations were performed with *GAUSSIAN 03*[21] and *MOLPRO 2000*.[22,23] The structure of CHClFI was calculated using the coupled-cluster theory with single and double excitations[24] augmented by a perturbational estimate of the effects of connected triple excitations (CCSD(T)).[25] In most cases, the CCSD(T) method is believed to yield a structure close to the equilibrium structure, provided the associated basis set is adequate and especially large enough.[26] This is not true for lower-level methods such as second-order Møller−Plesset perturbation theory (MP2).[27] To check the convergence, basis sets of different sizes will be used. For the first-row atoms (H, C, and F), the Dunning's correlation-consistent polarized valence

TABLE 1: Experimental and ab Initio Values of Rotational Constants, Centrifugal Distortion Constants, Quadrupole Coupling Constants (iodine and chlorine nuclei), and Spin−Rotation Constants (iodine nucleus) of $CH^{35}ClFI$ and $CH^{37}ClFI$[a]

	$CH^{35}ClFI$			$CH^{37}ClFI$		
constant/MHz	experimental	ab initio	(exptl −calcd/exptl)/%	experimental	ab initio	(exptl −calcd/exptl)/%
A	6278.651148(129)	6290.82[b]	−0.19	6192.865335(197)	6204.68[g]	−0.19
B	1474.152806(76)	1471.31[b]	0.19	1432.702503(173)	1429.90[g]	0.20
C	1224.416397(104)	1222.95[b]	0.12	1192.568955(193)	1191.10[g]	0.12
$\Delta_J\ 10^{+4}$	2.22294(52)	2.15[c]	3.25	2.22294[h]		
$\Delta_{JK}\ 10^{+5}$	−1.622(42)	−5.68[c]	−250.51[f]	−1.622[h]		
$\Delta_K\ 10^{+3}$	7.25410(103)	7.48[c]	−3.13	7.25410[h]		
$\delta_J\ 10^{+5}$	4.66127(133)	4.39[c]	5.71	4.66127[h]		
$\delta_K\ 10^{+4}$	9.3128(78)	8.86[c]	4.85	9.3128[h]		
$\Phi_K\ 10^{+8}$	1.847(116)			1.847[h]		
			Iodine Nucleus			
χ_{aa}	−1704.58015(252)	−1898.04[d]	−11.35	−1685.7418(42)		
χ_{bb}	838.57959	926.00[d]	−10.42	820.3798		
χ_{cc}	866.00056(244)	972.04[d]	−12.25	865.3620(47)		
χ_{ab}	699.7668(61)	792.63[d]	−13.27	731.8297(68)		
χ_{ac}	622.6878(160)	651.99[d]	−4.71	622.004(132)		
χ_{bc}	−140.4346(265)	−154.10[d]	−9.73	−148.7207(247)		
$C_{aa}\ 10^{+3}$	4.786(162)	3.6[d]	24.78	4.895(220)		
$C_{bb}\ 10^{+3}$	5.647(152)	5.3[d]	6.14	5.95(37)		
$C_{cc}\ 10^{+3}$	5.753(164)	5.5[d]	4.40	5.575(253)		
$C_{ab}\ 10^{+3}$	−2.17(34)			−2.18(46)		
			Chlorine Nucleus			
χ_{aa}	−13.3970(34)	−13.93[e]	−4.05	−11.5924(59)		
χ_{bb}	−15.4498	−14.84[e]	3.92	−11.2132		
χ_{cc}	28.8468(38)	28.78[e]	0.22	22.8056(67)		
χ_{ab}	-51.3943(117)	−50.30[e]	2.13	-40.5472(139)		
χ_{ac}	-22.7366(201)	−21.44[e]	5.70	-18.0474(234)		
χ_{bc}	-21.107(40)	−19.97[e]	5.38	-16.343(46)		

[a] Numbers in parentheses represent one standard deviation in units of the least significant digit. Relative uncertainties (exptl − calcd)/exptl are listed along the molecular parameters. [b] MP2/SDB-VTZ. [c] B3LYP/a′-VTZ-pp. [d] HF/6-311G**. [e] B3LYP/SDB-VTZ. [f] For explanation of discrepancy, see text. [g] Values derived from the ab initio structural parameters of $CH^{35}ClFI$. [h] Experimental values fixed from the corresponding values of $CH^{35}ClFI$.

TABLE 2: Definition of the Basis Set Functions Used in ab Initio Calculations of CHClFI

	triple-ζ quality				quadruple-ζ quality	
	a′-VTZ-pp	eef	SDB−VTZ	ref	SDB−VQZ	ref
H	cc-pVTZ	27	cc-pVTZ	27	cc-pVQZ	27
C	cc-pVTZ	27	cc-pVTZ	27	cc-pVQZ	27
F	aug-cc-pVTZ	39	cc-pVTZ	27	cc-pVQZ	27
Cl	cc-pV(T+d)Z	28	cc-pV(T+d)Z	28	cc-pV(Q+d)Z	28
I	cc-pVTZ-pp	40	SDB-cc-pVTZ	31	SDB-cc-pVQZ	30

triple-ζ basis sets[28] were used. For chlorine, which is a second-row atom, these standard basis sets give rise to nonnegligible errors. For this reason, the newly devised cc-pV(T+d)Z[29] was used. Finally, for iodine, the correlation-consistent polarized valence basis set with the Stuttgart−Dresden−Bonn (SDB) relativistic effective core potential,[30] SDB-cc-pVTZ[31,32] was used. This compound basis set is denoted SDB-VTZ hereafter (see Table 2 for the detail of the basis sets used). All calculations have been carried out correlating only valence electrons (frozen core approximation). Nondynamical electron correlation is not overly important, as concluded from the coupled-cluster T_1 diagnostic,[26] which is only 0.011. Therefore, CHClFI is expected to be well-described by single-reference coupled-cluster wave functions.

As convergence is obviously not achieved at the triple-ζ level, the larger SDB-VQZ (see Table 2) was also used but only at the correlated level of MP2 theory. There is indeed a large body of published evidence which indicates that the basis set effects are similar to the superior CCSD(T) level, and this significantly reduces the computational costs. The derived CCSD(T)/SDB-VQZ bond lengths are still different from the corresponding equilibrium values, mainly because the core correlation has been neglected. However, this remaining error is known to be almost constant for a given bond and can, thus, be estimated by comparing the CCSD(T)/SDB-VQZ and equilibrium bond lengths of the corresponding CH_3X (X = F, Cl, I) molecules[20] whose structure is accurately known. The results are presented in Table 3 where they are compared with the structural parameters of Schwerdtfeger et al.[2] The best estimate of the equilibrium structure is given in Table 3 under heading r_e.

It has to be noted that the MP2/SDB-VTZ structure is close to the estimated equilibrium structure. This is not fortuitous. The errors arising from the truncation of the one-electron space (basis set) and from the approximate treatment in the N-electron space (method) are often of opposite directions, giving considerable scope for cancellation of errors. It is indeed well-established that, when the CCSD(T) calculations are not affordable, the MP2/VTZ level of theory represents a balanced level of description;[33,34] therefore, the MP2/VTZ method is generally the best method (as far a structure is concerned) when the more expensive CCSD(T)/VQZ method cannot be used. This conclusion will be supported by the comparison of the experimental and ab initio rotational constants reported below.

Our second objective was the prediction of the principal rotation constants, the centrifugal distortion corrections, and the hyperfine constants (quadrupole coupling and spin−rotation). Also, to have an idea of the relative intensity of the μ_a-, μ_b-, and μ_c-type spectra, the dipole moment components were calculated at different levels of theory. The values of the predicted molecular parameters are presented in Table 1, along with the corresponding experimental values. At first, the equilibrium rotational constants calculated at the MP2/VTZ level of the theory were used to predict the rotational structure of the ground state. It is indeed usually observed that, for rigid molecules (r_0 differing from r_e by 1%), the MP2/VTZ results are close to the experimental ground-state constant values. This was also subsequently verified for CHClFI.

TABLE 3: Structural Parameters of $CH^{35}ClFI$ and Corresponding Rotational Constants Obtained by ab Initio Calculations

	methods and basis set[a]							
	CCSD(T)[b]	B3LYP	MP2		CCSD(T)			
parameters	cc-pVDZ	a′-VTZ-pp	SDB-VTZ	SDB-VQZ	SDB-VTZ	SDB-VQZ [c]	offset[d]	r_e[e]
r_{C-I}/pm	218.9	217.59	214.69	213.99	216.57	215.87	1.0	214.87
r_{C-H}/pm	110.1	108.37	108.32	108.30	108.09	108.06	0.2	107.91
r_{C-F}/pm	135.9	135.21	134.96	134.94	134.81	134.79	0.3	134.53
r_{C-Cl}/pm	177.9	176.81	175.40	174.98	176.82	176.40	0.6	175.80
∠HCI/deg	107.1	106.71	107.09	107.26	107.11	107.28		107.28
∠ICF/deg	109.3	109.18	109.45	109.48	109.48	109.52		109.52
∠ICCl/deg	113.3	112.82	112.23	112.06	112.27	112.10		112.10
∠HCF/deg	109.6	109.60	109.65	109.57	109.82	109.74		109.74
∠HCCl/deg	108.1	108.73	108.63	108.76	108.44	108.56		108.56
∠FCCl/deg	109.4	109.73	109.73	109.66	109.67	109.59		109.59
A_e/MHz	6222.99	6258.07	6290.82	6303.03	6251.61	6257.56		6296.90
B_e/MHz	1405.27	1429.65	1471.31	1482.04	1446.49	1457.27		1469.39
C_e/MHz	1174.96	1192.86	1222.95	1230.90	1204.41	1212.09		1221.87

[a] See Table 2. [b] ref 2. [c] CCSD(T)/SDB-VQZ ≅ CCSD(T)/SDB-VTZ − [MP2/SDB-VTZ − MP2/SDB-VQZ]. [d] The offset was obtained by comparison between CCSD(T)/SDB-VQZ results and the experimental values for CH_3X (X = F, Cl, and I) molecules. [e] r_e = CCSD(T)/SDB-VQZ-offset.

TABLE 4: Experimental and ab Initio Values of Quadrupole Coupling Constants and Corresponding Asymmetry Parameters and Structural Parameters for CHClFI, CH_2I_2, CH_2ClI, and CH_3I

	$CH^{35}ClFI$		CH_2I_2		$CH_2I^{35}Cl$		CH_3I	
parameters	exptl[a]	ab initio[b]	exptl[c]	ab initio [b]	exptl [d]	ab initio [b]	exptl[e]	ab initio[b]
$\chi_{zz}^{(Cl)}$/MHz	−75.070(22)	−75.2			−69.3	−73.0		
$\chi_{yy}^{(Cl)}$/MHz	39.045(25)	39.0			37.5	37.4		
$\chi_{xx}^{(Cl)}$/MHz	36.025(35)	36.2			31.5	35.6		
$\eta^{(Cl)}$/MHz	0.04023(65)	0.0372			0.0866	0.0246		
$\chi_{zz}^{(I)}$/MHz	−2025.218(9)	−2244.6	−2030.11(49)	−2213.4	−1988.1(42)	−2162.9	−1940.413(72)	−1987.4
$\chi_{yy}^{(I)}$/MHz	1032.013(25)	1141.3	1036.66(18)	1111.7	1021.1(43)	1098.3	970.206(36)	993.7
$\chi_{xx}^{(I)}$/MHz	993.177(27)	1103.3	993.45(49)	1101.7	967.0(34)	1064.6	970.206(36)	993.7
$\eta^{(I)}$/MHz	0.01918(2)	0.0169	0.02129(26)	0.0045	0.0272(28)	0.0156	0.0000	0.0000
r(C−I)/pm		214.7	213.5	213.0	213.7	213.6	213.4	213.2
r(C−Cl)/pm		175.4			177.4	176.0		
∠HCI/°		107.08		107.58		106.95	107.62	107.94
∠ICCl/°		112.23			112.48	113.61		
∠HCCl/°		108.63			108.40	108.93		
∠ICI/°			113.90	115.07				

[a] This work. [b] MP2/SDB-VTZ for structure, HF/6-311G** for quadrupolar coupling tensors of iodine, and B3LYP/SDB-VTZ for quadrupolar coupling tensors of chlorine. [c] ref 44. [d] ref 43. [e] ref 20 for structural parameters and ref 14 for quadrupolar coupling constants.

Many efforts were put into the calculation of the quartic centrifugal distortion constants in order to facilitate the prediction and assignment of the high J and K_a transitions. The harmonic force field is required to calculate the quartic centrifugal distortion constants. Because the CCSD(T) method would be extremely expensive in computer time (and memory), the density functional theory was used instead with the Becke[35] three parameter hybrid exchange functional and the Lee−Yang−Parr correlation functional[36] (B3LYP). This method is known to be inexpensive and remarkably accurate from the prediction of harmonic force fields.[37,38] For this calculation, diffuse functions were used for fluorine (aug-cc-p-VTZ),[39] and the small-core relativistic Pariser−Parr (PP) correlation-consistent basis set (cc-pVTZ-PP)[40] was used for iodine. This compound basis set is denoted a′-VTZ-pp in Table 2 (for completeness, the B3LYP structure is given in Table 3). The calculated centrifugal distortion constants obtained using the B3LYP harmonic force field are given in Table 1, and their values are discussed in the next section.

A purely empirical approach was followed for the calculation of the hyperfine constants (quadrupole coupling and spin−rotation). These constants were initially calculated for methyl halides, CH_3X (X = Cl, I) using different levels of theory. The method which gave the smallest error was used to calculate the constants of each atom of CHClFI separately. Calculations on CH_3Cl and CH_3I showed that reliable quadrupole tensors were obtained with the B3LYP/cc-pV(T+d)Z and the HF/6-311G** levels of theory for Cl and I, respectively. The results are listed in Table 4 for CH_3I and also for CH_2I_2 and CH_2ICl. For CH_3Cl, the ab initio values are as follows: $\chi_{zz}^{(Cl)} = -73.0$ MHz, $\chi_{xx}^{(Cl)} = \chi_{yy}^{(Cl)} = 36.5$ MHz, to be compared to the experimental values of $\chi_{zz}^{(Cl)} = -74.74$ MHz and $\chi_{xx}^{(Cl)} = \chi_{yy}^{(Cl)} = 37.37$ MHz.[41] The ab initio results are satisfactory for the iodine atom and surprisingly accurate for the chlorine atom. Also, the results confirm these small experimental differences between the molecules of this halides series. Therefore, the same approach was used to calculate the hyperfine constants of CHClFI, with their predicted values being reported in Table 1.

The permanent electric dipole moment has been calculated for CHFClI at the MP2/SDB-VTZ, MP2/SDB-VTZ, and B3LYP/a′-VTZ-pp levels of theory (Table 5). The three levels of calculations give consistent results, indicating that the calculated dipole moment is likely to be reliable. Furthermore, this is strengthened by the fact that the MP2/SDB-VTZ dipole moment of CH_3I, calculated in this work, is in good agreement with the experimental value (Table 5). For CHClFI, we predicted that the three *a*-, *b*-, and *c*-type transitions should be observed on the pure rotation spectrum, with $\mu_a \approx \mu_b < \mu_c$.

Discussion

Rotational Constants and Structure. Table 1 shows a comparison between experimental and ab initio spectroscopic constants of the $CH^{35}ClFI$ and $CH^{37}ClFI$ isotopologs. An

TABLE 5: Experimental and ab Initio Values of Electric Dipole Moments for CHClFI and CH_3I

	$CH^{35}ClFI$			CH_3I	
parameter	B3LYP/a′-VTZ-pp	MP2/SDB−VTZ	MP2/SDB−VQZ	exptl[a]	MP2/SDB−VTZ
μ/D	1.08	1.33	1.32	1.64	1.62
$\lvert\mu_a\rvert$/D	0.29	0.23	0.23	0.00	0.00
$\lvert\mu_b\rvert$/D	0.20	0.21	0.23	0.00	0.00
$\lvert\mu_c\rvert$/D	1.14	1.30	1.28	1.64	1.62

[a] ref 46.

TABLE 6: Quadrupole Coupling Tensors in Their Principal Axis System of $CH^{35}ClFI$ and $CH^{37}ClFI$

	$CH^{35}ClFI$		$CH^{37}ClFI$	
parameter	Iodine nucleus	Chlorine nucleus	Iodine nucleus	Chlorine nucleus
$\chi_{zz/MHz}$[a]	−2025.218(9)	−75.070(22)	−2025.177(8)	−59.167(24)
$\chi_{yy/MHz}$[a]	1032.013(25)	39.045(25)	1031.977(23)	30.768(28)
$\chi_{xx/MHz}$[a]	993.177(27)	36.025(35)	993.200(25)	28.399(38)
η[b]	0.01918(2)	0.04023(65)	0.01915(2)	0.04005 (8)
$\theta_{z,a}$[c]/deg	161.1035(2)	132.335(7)	160.5824(2)	133.006(11)
$\theta_{C-X,a}$[d]/deg	160.6496	130.878	160.0682	131.551
$\theta_{z,b}$[c]/deg	103.9897(1)	47.021(4)	104.6718(2)	47.649(7)
$\theta_{C-X,b}$[d]/deg	104.8150	45.548	105.5242	46.172
$\theta_{z,c}$[c]/deg	77.5547(3)	73.392(14)	77.5644(2)	73.472(20)
$\theta_{C-X,c}$[d]/deg	77.8344	73.436	77.8108	73.518

[a] Eigenvalues of the experimental quadrupole coupling tensors (Table 1). The principal axis z was taken to be the most negative quadrupole coupling constant; x and y are chosen arbitrarily. [b] Asymmetry parameter $\eta = (\chi_{xx} - \chi_{yy})/\chi_{zz}$. [c] Angles calculated from the rotation of the experimental quadrupole coupling tensor to its principal axis system x, y, and z. [d] Angles between the C−X bond and the principal axes a, b, and c calculated at the MP2/SDB-VTZ level.

inspection of Table 3 shows that the MP2/SDB-VTZ rotational constants are the closest to the experimental ground-state constants. Discrepancies less than 1% were obtained for rotational constants (A, B, and C). This indicates that the equilibrium structure is close to the ground vibrational state structure, which was expected for such a heavy molecule. Since only two different isotopologs ($CH^{35}ClFI$ and $CH^{37}ClFI$) were investigated, the structural information directly available from the experimental data is limited. Nevertheless, the r_s[Cl] coordinates of $CH^{35}ClFI$ can be compared to those determined by ab initio calculations. The Kraitchman equations[12] gave $|a_{Cl}| = 223.5$ pm, $|b_{Cl}| = 76.3$ pm, and $|c_{Cl}| = 5.3$ pm (where x_{Cl} and $x = a, b, c$ are the Cartesian coordinates in the a, b, c principal axis system). These results are in good agreement with the ab initio equilibrium values calculated at the MP2/SDB-VTZ level of theory: $a_{Cl} = -222.8$ pm, $b_{Cl} = -76.3$ pm, and $c_{Cl} = -6.0$ pm.

The centrifugal distortion constants show higher discrepancies, around 5%. The relative difference of 250% on the Δ_{JK} constant is due to accidental cancellation of same-order terms ($\Delta_{JK} = {}^3/_8(\tau_{bbbb} + \tau_{aaaa}) - {}^1/_4(\tau_{aacc} + \tau_{bbcc} + \tau_{ccaa}) = -0.6452$ kHz + 0.5883 kHz = −0.0568 kHz for $CH^{35}ClFI$).

Hyperfine Constants. At first, it should be noted that usually a unique set of signs for the off-diagonal elements of the quadrupole tensor cannot be experimentally determined. Indeed, Bauder and co-workers showed that, if unaltered, the following sign combinations give rise to identical spectra:[3]

$$\Pi^{(I)} = \mathrm{sign}(\chi_{ab}{}^{(I)}\chi_{ac}{}^{(I)}\chi_{bc}{}^{(I)}) \quad (9)$$

$$\Pi^{(Cl)} = \mathrm{sign}(\chi_{ab}{}^{(Cl)}\chi_{ac}{}^{(Cl)}\chi_{bc}{}^{(Cl)}) \quad (10)$$

$$\Pi_{ab} = \mathrm{sign}(\chi_{ab}{}^{(I)}\chi_{ab}{}^{(Cl)}) \quad (11)$$

$$\Pi_{ac} = \mathrm{sign}(\chi_{ac}{}^{(I)}\chi_{ac}{}^{(Cl)}) \quad (12)$$

$$\Pi_{bc} = \mathrm{sign}(\chi_{bc}{}^{(I)}\chi_{bc}{}^{(Cl)}) \quad (13)$$

However, in the present work, we also have used the quadrupole coupling tensors $\chi^{(I)}$, from CH_3I,[14] and $\chi^{(Cl)}$, from CH_3Cl.[15] By orienting these two tensors in the frame of CHClFI (see the preliminary analysis), we were able to obtain the off-diagonal elements with the correct signs. Indeed, in the rotation of an axis system, the values and the signs of the three Euler angles are determined. Therefore, the spectrum analysis gave us accurate experimental values, with the correct signs for the off-diagonal elements. These are in agreement with the corresponding signs of the ab initio calculations.

The ab initio calculations performed on $CH^{35}ClFI$ for the quadrupole coupling tensors were very satisfactory, especially in the case of the iodine nucleus. Indeed, the average of the relative uncertainties for both the diagonal and the off-diagonal components is 10.3%, which is an excellent result for a heavy nucleus such as iodine (Table 1).

The quality of the experimental and ab initio results illustrated above allows a discussion on the nature of the interactions of the nuclear quadrupoles and the field gradients for both halogen nuclei. Two independent quantities completely characterize the quadrupolar coupling tensor in its principal axis system: the χ_{zz} component of the tensor, which measures the quadrupolar coupling in the bond direction, and the asymmetry parameter $\eta = (\chi_{xx} - \chi_{yy})/\chi_{zz}$, which measures the deviation of the field-gradient tensor from axial symmetry.[42] The principal elements χ_{xx}, χ_{yy}, and χ_{zz} of the quadrupole coupling tensors along with their respective uncertainties are given for $CH^{35}ClFI$ and $CH^{37}ClFI$ in Table 6. These elements were calculated by diagonalizing the quadrupole coupling tensors expressed in the a, b, c principal axis system (see Table 1). As shown in Table 6, the asymmetry parameters values of $CH^{35}ClFI$ and $CH^{37}ClFI$ are very small, especially for the iodine tensors. It indicates that the z principal axis nearly coincides with the carbon−halogen bond (C−X; X = I, Cl). CHClFI behaves like most of the molecules with one or several carbon−halogen bonds: The deviation from an axial charge distribution around the halogen nucleus is very weak.[3,43,44] The comparison between the $\theta_{z,i}$ and $\theta_{C-X,i}$ angles confirms this point (Table 6). These are calculated in two independent ways. The angles $\theta_{z,i}$ are directly deduced from the rotation of the experimental quadrupole coupling tensor to its principal axis system. They correspond to the angles

between the *z* principal axis of the quadrupole tensor supposed in the direction of the bond and the *a*, *b*, and *c* principal inertial axes. The angles $\theta_{C-X,i}$ between the C−X bond (with X = I or Cl) and the *a*, *b*, and *c* principal inertial axes are deduced from the ab initio atomic coordinates. The near-equality between the $\theta_{z,i}$ and $\theta_{C-X,i}$ values indicates the closeness coincidence between the C−X bond and the *z* axis of the quadrupole coupling tensor.

Comparison of the χ_{zz} principal elements of the quadrupole coupling tensors between $CH^{35}ClFI$ and $CH^{37}ClFI$ shows consistent results. In the case of the iodine nucleus and within the uncertainty (three times the quoted standard deviation), the tensor is completely insensitive to the differences between the two chlorine isotopologs. In the case of the chlorine nucleus, the ratio $\chi_{zz}(^{35}Cl)/\chi_{zz}(^{37}Cl) = 1.268\,78(69)$ is in excellent agreement with the experimental value obtained in BrCl (1.268 89(3)).[45]

To go one step further in the analysis of the carbon−halogen bonds, the four methyl halides CHClFI, CH_2I_2, CH_2ClI, and CH_3I have been considered. In addition to the experimental $\chi^{(I)}$ and $\chi^{(Cl)}$ values, Table 4 displays the experimental values of $\eta^{(I)}$ and $\eta^{(Cl)}$. For all these molecules, the asymmetry parameters are very small, and the values of the principal elements of the quadrupole coupling tensors differ only by a few percent.

From both the experimental and ab initio values listed in Table 4, we observed that $\chi_{zz}^{(I)}(CH_2I_2) \approx \chi_{zz}^{(I)}(CHClFI) > \chi_{zz}^{(I)}(CH_2ClI) > \chi_{zz}^{(I)}(CH_3I)$. To interpret this result, we calculated structural parameters of the carbon−halogen bond (lengths and angles) using the second-order perturbational method MP2/SDB-VTZ. Structural data are shown in Table 4. Unfortunately, no conclusion can be taken from the lengths and the angles implied in the carbon−halogen bond for CHClFI, CH_2I_2, CH_2ClI, and CH_3I molecules.

Finally, it should be noted that the spin−rotation constants calculated at the HF/6-311G** level of theory are in good agreement with those determined experimentally.

Molecular Electric Dipole Moments. Although nuclear quadrupole coupling is sensitive to the charge distribution near the coupling nucleus, the dipole moment strongly depends on the charge distribution over the entire molecule. For this reason, dipole moments of polyatomic molecules are more difficult to interpret quantitatively than nuclear quadrupole coupling tensors.[12] By assuming qualitatively no drastic change in bond character from one methyl halide to another, the dipole moments defined for each bond are vectorially additive. This approach allows the understanding of the relative dipole moment values in the methyl halides. As an example, the dipole moment module of a symmetric top like CH_3I, containing only one halogen nucleus, is stronger than the corresponding value of an asymmetric top like CHClFI, in which the dipole moments along the carbon−halogen bonds compensate each other.

Conclusion

We have recorded the pure rotational spectrum of the chiral molecule CHClFI in the centimeter- and millimeter-wave region. A complete set of spectroscopic parameters, including the rotational and centrifugal distortion constants, all the elements of the quadrupole coupling tensor for the iodine and chlorine nuclei, and spin−rotation constants for the iodine nucleus, were fitted to the experimental frequencies within the experimental accuracy. All these constants and structural parameters were also obtained using sophisticated ab initio calculations. A systematic comparison with the experimental data shows that the discrepancies are small, within the precision of the level of the theory. The experimental quadrupole coupling tensors have been transformed to their own principal axis system. The asymmetry parameters were very small, indicating nearly cylindrical symmetry of the C−Cl and C−I bonds. Their limited accuracy did not justify further interpretation.

The ground-state rotational constants determined in this work will allow the high-resolution infrared spectrum to be obtained and analyzed. Of particular interest is the selection of a well-isolated IR transition associated with the C−F stretching vibration (fundamental or first overtone band). Such a transition, predicted at 1081.4 cm^{-1}, would be a good candidate to provide evidence of the parity violation effect between the two enantiomers of CHClFI by a saturation spectroscopy experiment. This effect is predicted to be proportional to Z.[5] Alternative larger molecules have been proposed for future studies; indeed, Schwerdtfeger and Bast recently suggested the investigation of the vibrational spectrum of organometallic compounds containing an Os═O or a Re═O double bond for which the parity violation effects would be on the order of 1 Hz.[47] However, the high-resolution spectroscopy of these molecules will present a significant challenge.

Acknowledgment. Part of this work was supported by the Institut du Développement et des Ressources en Informatique Scientifique (IDRIS), contract 41715. Fabrice Willaert is thanked for the MMW measurements.

Supporting Information Available: The frequencies of the assigned microwave and millimeter-wave lines for the two chlorine isotopologs, along with the observed minus calculated values, are collected in the Supporting Information (Tables 1S and 2S). This material is available free of charge via the Internet at http://pubs.acs.org.

References and Notes

(1) Laerdahl, J. K.; Schwerdtfeger, P.; Quiney, H. M. *Phys. Rev. Lett.* **2000**, *84*, 3811.
(2) Schwerdtfeger, P.; Laerdahl, J. K.; Chardonnet, C. *Phys. Rev. A* **2002**, *65*, 42508.
(3) Bauder, A.; Beil, A.; Luckhaus, D.; Müller, F.; Quack M. *J. Chem. Phys.* **1996**, *106*, 7558.
(4) Daussy, C.; Marrel, T.; Amy-Klein, A.; Nguyen, C.; Bordé, C.; Chardonnet, C. *Phys. Rev. Lett.* **1999**, *83*, 1554.
(5) Ziskind, M.; Daussy, C.; Marrel, T.; Chardonnet, C. *Eur. Phys. J. D* **2002**, *20*, 219.
(6) Quack, M.; Stohner, J. *J. Chem. Phys.* **2003**, *119*, 11228.
(7) Amy-Klein, A.; Chardonnet, C. Private communication, 2004.
(8) Crassous, J.; Jiang, Z.; Schurig, V.; Polavarapu, P. L. *Tetrahedron: Asymmetry* **2004**, *15*, 1995.
(9) Li, D. B.; Ng, S. C.; Novak, I. *Tetrahedron* **2002**, *58*, 5923.
(10) Kassi, S.; Petitprez, D.; Wlodarczak, G. *J. Mol. Struct.* **2000**, *517−518*, 375.
(11) Kroto, H. W. *Molecular rotation spectra*; Dover Publications: New York, 1975.
(12) Gordy, W.; Cook, R. L. *Microwave Molecular Spectra*; Wiley: New York, 1984.
(13) Thaddeus, P.; Krisher, L. C.; Loubser, J. H. N. *J. Chem. Phys.* **1964**, *40*, 257.
(14) Dubrulle, A.; Burie, J.; Boucher, D.; Herlemont, F.; Demaison, J. *J. Mol. Spectrosc.* **1981**, *88*, 394.
(15) Wlodarczak, G.; Boucher, D.; Bocquet, R.; Demaison, J. *J. Mol. Spectrosc.* **1990**, *139*, 11.
(16) Pickett, H. M. *J. Mol. Spectrosc.* **1991**, *148*, 371.
(17) Bieròn, J.; Pyykkö, P.; Sundholm, D.; Kellö, V.; Sadlej, A. J. *Phys. Rev. A* **2001**, *64*, 52507.
(18) Sundholm, D.; Olsen, J. *J. Chem. Phys.* **1993**, *98*, 7152.
(19) Oka, T. *J. Chem. Phys.* **1966**, *45*, 752.
(20) Demaison, J.; Margulès, L.; Boggs, J. E. *Struct. Chem.* **2003**, *14*, 159.
(21) Frisch, M. J.; Trucks, G. W.; Schlegel, H. B.; Scuseria, G. E.; Robb, M. A.; Cheeseman, J. R.; Montgomery, Jr., J. A.; Vreven, T.; Kudin, K. N.; Burant, J. C.; Millam, J. M.; Iyengar, S. S.; Tomasi, J.; Barone, V.; Mennucci, B.; Cossi, M.; Scalmani, G.; Rega, N.; Petersson, G. A.;

Nakatsuji, H.; Hada, M.; Ehara, M.; Toyota, K.; Fukuda, R.; Hasegawa, J.; Ishida, M.; Nakajima, T.; Honda, Y.; Kitao, O.; Nakai, H.; Klene, M.; Li, X.; Knox, J. E.; Hratchian, H. P.; Cross, J. B.; Bakken, V.; Adamo, C.; Jaramillo, J.; Gomperts, R.; Stratmann, R. E.; Yazyev, O.; Austin, A. J.; Cammi, R.; Pomelli, C.; Ochterski, J. W.; Ayala, P. Y.; Morokuma, K.; Voth, G. A.; Salvador, P.; Dannenberg, J. J.; Zakrzewski, V. G.; Dapprich, S.; Daniels, A. D.; Strain, M. C.; Farkas, O.; Malick, D. K.; Rabuck, A. D.; Raghavachari, K.; Foresman, J. B.; Ortiz, J. V.; Cui, Q.; Baboul, A. G.; Clifford, S.; Cioslowski, J.; Stefanov, B. B.; Liu, G.; Liashenko, A.; Piskorz, P.; Komaromi, I.; Martin, R. L.; Fox, D. J.; Keith, T.; Al-Laham, M. A.; Peng, C. Y.; Nanayakkara, A.; Challacombe, M.; Gill, P. M. W.; Johnson, B.; Chen, W.; Wong, M. W.; Gonzalez, C.; Pople, J. A. *Gaussian 03*, Revision B.04; Gaussian, Inc., Wallingford CT, 2004.

(22) Werner, H.-J.; Knowles, P. J.; with contributions from Amos, R. D.; Bernhardsson, A.; Berning, A.; Celani, P.; Cooper, D. L.; Deegan, M. J. O.; Dobbyn, A. J.; Eckert, F.; Hampel, C.; Hetzer, G.; Korona, T.; Lindh, R.; Lloyd, A. W.; McNicholas, S. J.; Manby, F. R.; Meyer, W.; Mura, M. E.; Nicklass, A.; Palmieri, P.; Pitzer, R.; Rauhut, G.; Schütz, M.; Stoll, H.; Stone, A. J.; Tarroni, R.; Thorsteinsson, T. *MOLPRO 2000*, a package of ab initio programs. http://www.molpro.net/.

(23) Knowles, P. J.; Hampel, C.; Werner, H.-J. *J. Chem. Phys.* **2000**, *112*, 3106.

(24) Purvis, G. D.; Bartlett, R. J. *J. Chem. Phys.* **1982**, *76*, 1910.

(25) Raghavachari, K.; Trucks, G. W.; Pople, J. A.; Head-Gordon, M. *Chem. Phys. Lett.* **1989**, *157*, 479.

(26) Lee, T. J.; Scuseria, G. E. In *Quantum Mechanical Electronic Structure Calculations with Chemical Accuracy*; Langhoff, S. R., Ed.; Kluwer: Dordrecht, 1995; pp 47−108.

(27) Møller, C.; Plesset, M. S. *Phys. Rev.* **1934**, *46*, 618.

(28) Dunning, T. H., Jr. *J. Chem. Phys.* **1989**, *90*, 1007.

(29) Dunning, T. H., Jr.; Peterson, K. A.; Wilson, A. K. *J. Chem. Phys.* **2001**, *114*, 9244.

(30) Bergner, A.; Dolg, M.; Küchle, W.; Stoll, H.; Preuss, H. *Mol. Phys*. **1993**, *80*, 1431.

(31) Martin, J. M. L.; Sundermann, A. J. *J. Chem. Phys.* **2001**, *114*, 3408.

(32) Basis sets were obtained from the Extensible Computational Chemistry Environment Basis Set Database, Version 6/19/03, as developed and distributed by the Molecular Science Computing Facility, Environmental and Molecular Sciences Laboratory which is part of the Pacific Northwest Laboratory, P.O. Box 999, Richland, WA 99352, U.S.A., and funded by the U.S. Department of Energy. The Pacific Northwest Laboratory is a multiprogram laboratory operated by Battelle Memorial Institute for the U.S. Department of Energy under contract DE-AC06-76RLO 1830. Contact David Feller or Karen Schuchardt for further information.

(33) Helgaker, T.; Jørgensen, P.; Olsen, J. In *Molecular Electronic−Structure Theory*; Wiley: New York, 2002; Chapter 15.

(34) Helgaker, T.; Gauss, J.; Jørgensen, P.; Olsen, J. *J. Chem. Phys.* **1997**, *106*, 6430.

(35) Becke, A. D. *J. Chem. Phys.* **1993**, *98*, 5648.

(36) Lee, C. T.; Yang, W. T.; Parr, R. G. *Phys. Rev. B* **1988**, *37*, 785.

(37) Bauschlicher, C. W.; Ricca, A.; Partridge, H.; Langhoff, S. R. In *Recent Advances in Density Functional Methods*; Chong, D. P., Ed.; World Scientific: Singapore, 1997; p 165.

(38) Montgomery, J. A.; Frisch, M. J.; Ochterski, J. W.; Petersson, G. A. *J. Chem. Phys.* **1999**, *110*, 2822.

(39) Kendall, R. A.; Dunning, T. H., Jr.; Harrison, R. J. *J. Chem. Phys.* **1992**, *96*, 6796.

(40) Peterson, K. A.; Figgen, D.; Goll, E.; Stoll, H.; Dolg, M. *J. Chem. Phys.* **2003**, *119*, 11099.

(41) Man, H. T.; Butcher, R. J. *J. Mol. Spectrosc.* **1985**, *110*, 19.

(42) Lucken, E. A. C. *Nuclear quadrupole coupling constants*; Academic Press: London and New York, 1969.

(43) Okhoshi, I.; Niide, Y.; Takano, M. *J. Mol. Spectrosc.***1990**, *139*, 11.

(44) Kisiel, Z.; Pszczolkowsky, L.; Caminati, W.; Favero, P. G. *J. Chem. Phys.* **1996**, *105*, 1778.

(45) Legon, A. C.; Thorn, J. C. *Chem. Phys. Lett.* **1993**, *215*, 554.

(46) Gadhi, J.; Wlodarczack, G.; Legrand, J.; Demaison, J. *Chem. Phys. Lett.* **1989**, *156*, 401.

(47) Schwerdtfeger, P.; Bast, R. *J. Am. Chem. Soc.* **2004**, *126*, 1652.